Available online at www.sciencedirect.com
ScienceDirect
Journal of Magnetism and Magnetic Materials 308 (2007) 273–277
Journal of magnetism and magnetic materials
www.elsevier.com/locate/jmmm

Helical anisotropy and magnetoimpedance of CoFeSiB wires under torsional stress

C. Tannous[a,*], J. Gieraltowski[a], R. Valenzuela[b]

[a]UBO, LMB-CNRS FRE 2697, C.S. 93837 Brest, Cedex 29238, France
[b]Instituto de Investigaciones en Materiales, Universidad Nacional Autónoma de Mexico, P.O. Box 70-360, Coyoacan, Mexico D.F. 04510, Mexico

Received 5 January 2006; received in revised form 15 May 2006
Available online 28 June 2006

Abstract

Recent measurements of the magnetoimpedance (at a fixed frequency of 1 MHz) of cobalt-rich wires subjected to torsion stress show an asymmetry as a function of torsion angle stemming from residual anisotropies induced during wire fabrication. We interpret these measurements with a simple model based on the competition between a circumferential magnetic anisotropy and another one induced by torsional or residual stress. This allows extraction of the physical parameters of the wire and explains the positive and negative torsion cases. The agreement between theoretical and experimental results provides a firm support for the model describing the behavior of the anisotropy field versus static magnetic field for all torsion angles.

PACS: 75.50.Kj; 72.15.Gd; 75.30.Gw; 75.80.+q

Keywords: Amorphous magnetic wires; Giant magnetoimpedance; Magnetic anisotropy; Magnetostriction

1. Introduction

The giant magnetoimpedance effect (GMI) in amorphous ribbons, wires and thin films has become a topic of growing interest for a wide variety of prospective applications in storage information technology and sensors possessing high sensitivity and fast response [1,2].

Magnetoimpedance effect (MI) consists in the change of impedance introduced by a low-amplitude AC current I_{AC} flowing through a magnetic conductor under application of a static magnetic field H_{DC} (usually parallel to the direction of the AC current). The origin of this behavior is related to the relative magnetic permeability μ_r and the direction of the magnetic anisotropy field H_K. When MI measurements are performed on wires, injecting an AC current in the wire and applying a DC magnetic field H_{DC} along the wire axis, one probes the wire rotational permeability wire that controls the behavior of the MI.

Ordinarily, the MI curve is symmetric with respect to the DC magnetic field H_{DC} with a single (at $H_{DC} = 0$) or a double peak (when $H_{DC} = \pm H_{max}$), the anisotropy field of the wire being considered as the value of H_{max}. Applying a torsion stress to the wire alters its MI behavior versus field H_{DC} in a way such that one observes, for instance, a single peak only for positive stress and a double peak for negative stress.

Recent work by Betancourt and Valenzuela (BV) [3] tackled MI measurements of CoFeBSi wires subjected to torsion stress [4,5], at a fixed frequency of 1 MHz, obtaining the aforementioned asymmetry [6,7] of the MI profile with respect to torsion stress. Interpreting the asymmetry in terms of residual anisotropies induced during wire fabrication [3] leads to an effect that, respectively, counterbalances or enhances the wire circumferential anisotropy with positive or negative torsional stress.

The wires were prepared by the in-rotating water-quenching technique and have the nominal composition $(Co_{94}Fe_6)_{72.5}Si_{12.5}B_{15}$. Their typical dimensions are 10 cm in length and 120 μm for diameter. They possess a characteristic domain structure dictated by the sign of the

*Corresponding author. Tel.: +33 298 016228; fax: +33 298 017395.
E-mail address: tannous@univ-brest.fr (C. Tannous).

0304-8853/$ - see front matter © 2006 Elsevier B.V. All rights reserved.
doi:10.1016/j.jmmm.2006.05.028

magnetostriction coefficient λ_s^R which is expected to have a small value ($|\lambda_s^R| \sim 10^{-7}$ in these Cobalt-rich alloys). When λ_s^R is negative, an axially oriented magnetization core exists surrounded by circular domains [1,2], whereas in the opposite case, radially oriented magnetization states exist such as those observed in Fe-rich alloys [7]. After performing several measurements such as Barkhausen jump and magnetization reversal measurements [3], BV favor the negative sign for the λ_s^R coefficient and presence of helical anisotropy [4].

In this paper, a simple model for the anisotropy field, based on the competition between a fabrication-induced circumferential anisotropy and a torsion-induced one with presence of fabrication-induced residual torsional stress, is proposed. This model allows the extraction of the relevant physical parameters of the wire and explains the observed behavior in the cited work [3] as a function of the static magnetic field for all torsion angles.

2. Theory

In order to reveal the residual stress within the wires, positive and negative torsion stress [4] are applied and the effect is analyzed with MI response. Following the work of Favieres et al. [8] on cylindrical CoP amorphous multilayers electrodeposited on copper wires, we use a stress-induced easy axis making an arbitrary angle δ_T [4] with the circumferential direction (see Fig. 1). We extend this model to include the presence of residual torsion stress induced by fabrication. The total magnetoelastic energy in presence of applied and residual torsional stress (σ_r) is

$$E = K_c \sin^2(\theta) + \frac{3}{2}\lambda_s^R(\sigma + \sigma_r)\sin^2(\delta_T - \theta), \quad (1)$$

where K_c is the fabrication-induced circumferential anisotropy of the wire and λ_s^R the rotational saturation magnetostriction constant [9] (see Fig. 1). We are in the linear case where the magnetoelastic energy is proportional to stress σ. Our energy functional does not include demagnetization nor Zeeman terms originating from the DC field H_{DC} applied along the wire axis. Energy due to the AC circular field H_{AC} created by the injected AC current I_{AC} is neglected. The anisotropy field as a function of stress is determined by identifying it, experimentally, with the value of the DC field H_{max} where the MI curve displays a peak. Previously Makhnovskiy et al. [10] introduced explicitly these terms in the energy functional with a single helical anisotropy [4] term in contrast with our work dealing with several competing (fabrication and torsion-induced) anisotropies. The stress σ (on the surface of the wire) is related to the torsion angle δ through:

$$\sigma = (Ga\delta)/l, \quad (2)$$

where G is the shear modulus, a is the radius of the wire and l the length (see Fig. 2). In general, σ has a radial dependence since the wire has an inner core with an axial magnetization surrounded by circular domains [1,2] when λ_s^R is small and negative. We neglect such dependence and consider, for simplicity, the value of stress on the surface [11] of the wire. Introducing the saturation magnetization of the samples M_s (measured with a vibrating sample magnetometer [3] as $\mu_0 M_s = 0.8\,\mathrm{T}$), the energy may be rewritten as

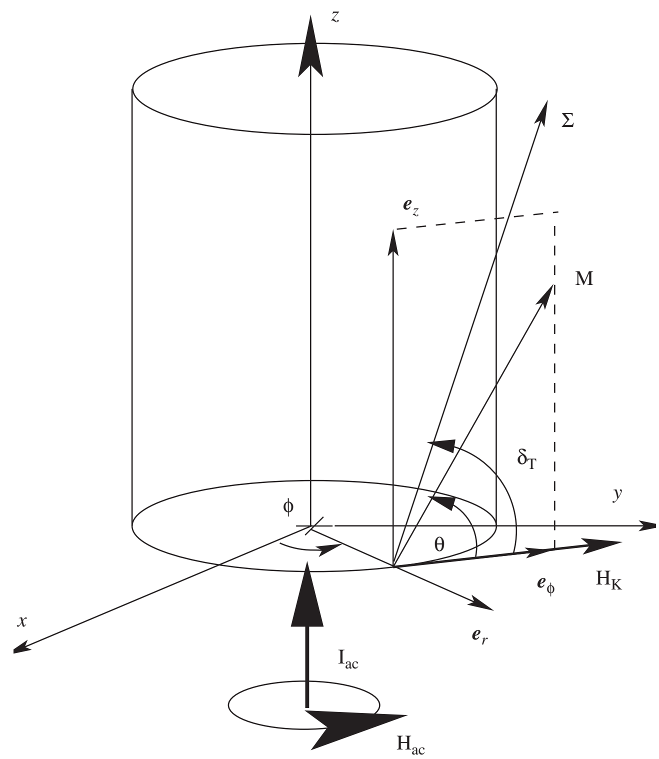

Fig. 1. Geometry of the anisotropy and stress-induced easy axis. The circumferential anisotropy axis induced by fabrication is along $\mathbf{e}_\phi$ and the torsion stress-induced easy axis $\mathbf{\Sigma}$ makes an angle δ_T with $\mathbf{e}_\phi$. The zero-stress circular anisotropy field H_K is along $\mathbf{e}_\phi$. In the helical anisotropy case, the magnetization $\mathbf{M}$ lies in the $\mathbf{e}_\phi$, $\mathbf{e}_z$ plane making a non-zero angle θ with the circumferential basis vector $\mathbf{e}_\phi$, otherwise, both the magnetization $\mathbf{M}$ and anisotropy axis lie in the $\mathbf{e}_r$, $\mathbf{e}_\phi$ plane.

$$E = (M_s/2)[H_K \sin^2(\theta) + H_\sigma \sin^2(\theta - \delta_T)]. \quad (3)$$

This shows that we have a competition between a circumferential anisotropy field $H_K = 2K_c/M_s$ and a torsion stress-induced one (called henceforth twist field including the residual stress) $H_\sigma = 3\lambda_s^R(\sigma + \sigma_r)/M_s$. Using a Stoner–Wohlfarth approach [12,13], this amounts to rotate the astroid equation from a set of perpendicular fields H_x, H_y:

$$H_x^{2/3} + H_y^{2/3} = H_K^{2/3} \quad (4)$$

to another by an angle θ^* resulting in another astroid. This angle is the same that gives the new equilibrium orientation of the magnetization and is simply obtained from the condition minimizing the energy, i.e. $[\partial E/\partial\theta]_{\theta=\theta^*} = 0$. We obtain

$$\tan(2\theta^*) = \frac{H_\sigma \sin(2\delta_T)}{H_K + H_\sigma \cos(2\delta_T)}. \quad (5)$$

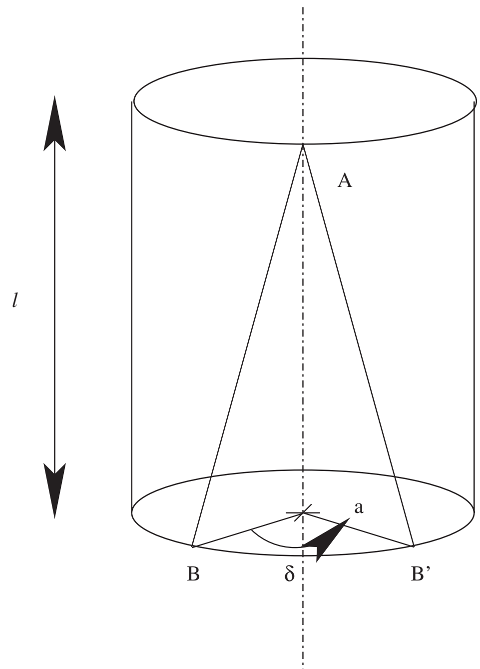

Fig. 2. Applying a torsion stress to a wire moves the point B to B' by angle δ. The deformation is the displacement per unit length, i.e. $\varepsilon = BB'/l = a\delta/l$ where l is the length of the wire. By Hooke's law, stress and deformation are related by the shear modulus G, hence $\sigma = G\varepsilon = G(a\delta/l)$.

Using this expression of θ^*, the resulting anisotropy field H^* is written as

$$H^* = \sqrt{H_K^2 + H_\sigma^2 + 2H_K H_\sigma \cos(2\delta_T)}. \tag{6}$$

The total energy after this transformation is written as

$$E = (M_s/2)[H^* \sin^2(\theta - \theta^*) - H^* \sin^2(\theta^*) + H_\sigma \sin^2(\delta_T)] \tag{7}$$

indicating the presence of helical [4] anisotropy (since we have an angle δ_T in general different from 0° and 90°) resulting from the competing circumferential and torsion (applied + residual) induced one. In fact we ought to find from the MI experiment the angles bounding the value of δ_T.

The MI peak value versus field and torsion angle should correspond to the anisotropy field H^* given by the above formula (Eq. (6)) as explored in the next section.

3. Numerical procedure

The MI maximum value field H_{max} is to be fitted to the theoretical expression of H^*. The latter depends on four parameters, H_K the zero-stress circumferential anisotropy field, $b = 3\lambda_s^R/M_s$ the normalized magnetostriction constant, the angle δ_T and the residual torsional stress σ_r. These can be reduced to three by normalising all quantities by H_K.

We use a procedure based on a least squares minimization procedure of the curve H^* versus σ to the set of experimental measurements $[\sigma_i, y_i]_{i=1,n}$ where $y_i = H^*(\boldsymbol{\alpha}; \sigma_i)$. $\boldsymbol{\alpha}$ represents the set of parameters b, δ_T and σ_r. The slope of the curve H^* versus σ that appears to be linear is used in the fitting. This choice is sufficient for the description of the method we use, nonetheless our algorithm allows us to select any coherent set of criteria we choose to fit the data.

Hence the couple of minimum equations for the data points and the slope are

$$\frac{1}{n}\sum_{i=1}^{n}[H^*(\boldsymbol{\alpha}; \sigma_i) - y_i]^2 \tag{8}$$

$$\left|\frac{1}{n}\sum_{i=1}^{n}\frac{[b^2(\sigma_i + \sigma_r) + bH_K\cos(2\delta_T)]}{H^*(\boldsymbol{\alpha}; \sigma_i)} - s_e\right|, \tag{9}$$

where s_e is the overall experimental slope. The fitting method is based on the Broyden algorithm which is the generalization to higher dimension of the one-dimensional secant method [14] and allow us to determine in principle two unknowns out of three b, σ_r and δ_T. Broyden method is chosen because it can handle underdetermined problems (since we have two equations and three unknowns).

We consider two cases:

Case A: Absence of residual stress ($\sigma_r = 0$), then H_K is determined as $H_K = H^*(\boldsymbol{\alpha}; 0)$ and b, δ_T are obtained with Broyden algorithm.

Case P: Presence of residual stress, then H_K is a normalising parameter and b, σ_r are evaluated with Broyden algorithm.

The parameter $Ga/l = 60.82\,\text{MPa/rad}$ is obtained directly by averaging over the torsion angles and the torsion stress as done in Ref. [3]. Using a wire radius of $a = 60\,\mu\text{m}$ and a length of $l = 10\,\text{cm}$, we obtain $G = 100\,\text{GPa}$ which is a little different from the value used in Ref. [3] (60 GPa).

The fitting shown in Fig. 3 (corresponding to case P as explained in the next section) allows us to predict the anisotropy field H^*, in the negative stress torsion case, from the experimental results of MI measurements; that is interesting enough, since the single peak is dominant (at $H_{DC} = 0$) and the double peak is barely noticeable in the MI curve versus H_{DC}. As an example, we can infer that the anisotropy field H^* is zero for a negative value of stress $\sigma \sim -150\,\text{MPa}$.

4. Results and discussion

The fitting procedure in case A, discriminates among the positive and negative λ_s^R values in favor of the negative value (implying presence of circular magnetization pattern in the wire). The fitting quality (equivalent to a χ^2 test) is 0.094 when $b = 1.39\,\text{(A/m)/MPa}$ (roughly equal to the slope of H^* versus σ) the angle δ_T is almost 180° and $\lambda_s^R = 4.68 \times 10^{-7}$. On the other hand, the fitting quality is 1.8×10^{-3}, with $b = 1.70$ (A/m)/MPa, and $\delta_T \sim 0°$. In this case $\lambda_s^R = -4.55 \times 10^{-7}$ agreeing with the value found by BV [3].

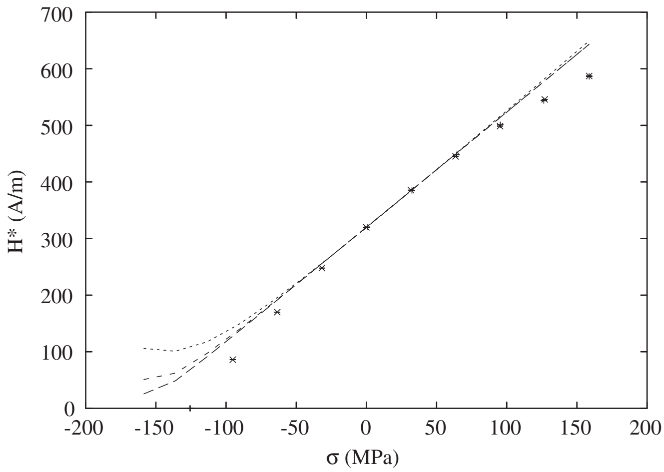

Fig. 3. Experimental results of the anisotropy field H^* versus stress as obtained by BV [3] from the field value of H_{DC} at MI peak value and theoretical lines for variable circular anisotropy field H_K at zero-stress. As H_K is decreased from 100 A/m (upper line) to 50 A/m and finally 25 A/m (lowest line) we get a weaker tapering off of the line for negative stress σ and better fitting of the experimental results. The residual torsion stress is ~150 MPa.

In spite of the successful fit, the result is not acceptable for at least two reasons: firstly, with torsional stress the angle δ_T should be at least 45° (or between 45° and 90° as in Favieres et al. [8] and Makhnovskiy et al. [10]), Secondly the zero-stress anisotropy field H_K ($H_K = 320$ (A/m) [3] is too large for these wires (For Cobalt-rich wires H_K is on the order of a few tens of A/m).

Then we move on to discuss the next case P. Starting with $H_K = 100$ A/m, we perform Broyden minimization obtaining: $b = 2.13$ (A/m)/MPa yielding $|\lambda_s^R| = 7.13 \times 10^{-7}$ while $\sigma_r = 142.4$ MPa. For $H_K = 50$ A/m we obtain: $b = 2.05$ (A/m)/MPa yielding $|\lambda_s^R| = 6.87 \times 10^{-7}$ while $\sigma_r = 154.1$ MPa. It is remarkable to notice that the fitting curve tapers off for negative stress (see Fig. 3) while getting better for smaller values of H_K. For $H_K = 25$ A/m we obtain: $b = 2.03$ (A/m)/MPa yielding $|\lambda_s^R| = 6.83 \times 10^{-7}$ while $\sigma_r = 156.5$ MPa.

The value $|\lambda_s^R| = 6.83 \times 10^{-7}$ is slightly larger than found previously by BV. However, we agree with BV [3] interpretation of the MI asymmetry in terms of a residual torsion stress (~150 MPa) that is enhanced or counterbalanced (since $H^* = 0$ for $\sigma = -150$ MPa) with an applied positive or negative torsional stress. The origin of the asymmetry was interpreted by Freijo et al. [15] on the basis of the exchange coupling between the wire axis core, axially magnetized, and the rest of the volume carrying a circular magnetization. During cooling the tubular domain wall structure induced between both regions retain an anisotropy equivalent to the observed helical.

We conclude that our results are similar to those obtained with the A case and agree as well with those obtained by BV despite the use in both cases of the linear fit: $H^* = H_K + b\sigma$ that allows to extract from the slope of the H^* versus σ the magnetostriction coefficient with the formula [16]:

$$\lambda_s^R = -(\mu_0 M_s/3)(dH^*/d\sigma). \tag{10}$$

In order to examine the general case with $\cos(2\delta_T) \neq \pm 1$, we observe that when the magnitude of the twist field H_σ is small with respect to the zero-stress anisotropy field H_K one may expand, to fourth order (for instance), the anisotropy field H^* with respect to σ obtaining

$$H^*/H_K = 1 + \frac{H_\sigma}{H_K}\cos(2\delta_T) + \frac{1}{2}\left[\frac{H_\sigma}{H_K}\right]^2 \sin^2(\delta_T) - \frac{1}{2}\left[\frac{H_\sigma}{H_K}\right]^3 \cos(2\delta_T)\sin^2(\delta_T) + O(\sigma^4). \tag{11}$$

One may also derive a similar expansion for λ_s^R as a function of σ [16]. Using the above relationship Eq. (10), one gets

$$\lambda_s^R = -(\mu_0 M_s b/3)\left\{\cos(2\delta_T) + \frac{H_\sigma}{H_K}\sin^2(\delta_T) - \frac{3}{2}\left[\frac{H_\sigma}{H_K}\right]^2 \cos(2\delta_T)\sin^2(\delta_T) + O(\sigma^3)\right\}. \tag{12}$$

Previously, this kind of expansion has been performed by several workers and particularly by Zhukov et al. [17] who made also a fitting of the expansion coefficients as a function of frequency. This might be included easily in our approach by letting H_σ vary with frequency.

Generally speaking, the linear regime $H^* = H_K \pm b\sigma$ should not be observed when the angle δ_T is different from 0° and 90° (± an integer multiple of 90°). Then the relationship $H^* = \sqrt{H_K^2 + H_\sigma^2 + 2H_K H_\sigma \cos(2\delta_T)}$ should apply and when the twist field is small ($H_\sigma \ll H_K$), the above expressions Eqs. (11), and (12) apply.

Experiments versus frequency involving wires with off-wire axis torsion stress conditions ought to be done in order to test the general non-linear case (where H_σ not necessarily being very small with respect to H_K), and precision in measuring H^* versus σ should be increased (in the positive torsion angle case of BV [3]) in order to be able to locate accurately the peak of the MI versus field H_{DC} and test the above formula. This work is in progress.

References

[1] K. Mohri, T. Uchiyama, L.P. Shen, C.M. Cai, L.V. Panina, Y. Honkura, M. Yamamoto, IEEE Trans. Magn. 38 (2002) 3063.
[2] L.V. Panina, K. Mohri, T. Uchiyama, M. Noda, K. Bushida, IEEE Trans. Magn. 31 (1995) 1249.
[3] I. Betancourt, R. Valenzuela, Appl. Phys. Lett. 83 (2003) 2022.
[4] Helical anisotropy is generally accounted for by introducing an anisotropy axis making an angle $\psi(45° \leqslant \psi < 90°)$ with the wire axis (see for instance Ref. [10]). Note that torsion stress is also called helical because it is modeled as tensile and compressive stresses acting perpendicularly on the wire surface with an angle of 45° with the wire axis [5].
[5] M.J. Sablik, D.C. Jiles, IEEE Trans. Magn. 35 (1999) 498.

[6] J.M. Blanco, A. Zhukov, J. Gonzalez, J. Appl. Phys. 87 (2000) 4813, see also J.M. Blanco, A. Zhukov, J. Gonzalez, J. Phys. D: Appl. Phys. 32 (1999) 3140.
[7] G.H. Ryu, C.S. Yu, C.G. Kim, I.H. Nahm, S.S. Yoon, J. Appl. Phys. 87 (2000) 4828.
[8] C. Favieres, C. Aroca, M.C. Sanchez, V. Madurga, J. Appl. Phys. 87 (2000) 1889.
[9] The saturation magnetostriction constants in the tensile case (λ_s^T) and in the torsion case (λ_s^R) are, in general, different for a crystalline material. In amorphous materials $\lambda_s^R \sim \lambda_s^T$.
[10] D.P. Makhnovskiy, L.V. Panina, J. Mapps, Phys. Rev. B 63 (14) (2001) 144424.
[11] V. Raposo, J.M. Gallego, M. Vazquez, J. Magn. Magn. Mater. 242–245 (2002) 1435.
[12] E.C. Stoner, E.P. Wohlfarth, Philos. Trans. R. Soc. London A 240 (1948) 599.
[13] L.D. Landau, E.M. Lifshitz, Electrodynamics of Continuous Media, Pergamon, Oxford, 1975, p. 195.
[14] W.H. Press, W.T. Vetterling, S.A. Teukolsky, B.P. Flannery, Numerical Recipes in C: The Art of Scientific Computing, Second Edition, Cambridge University Press, New York, 1992, p. 389.
[15] J.J. Freijo, A. Hernando, M. Vazquez, A. Méndez, V.R. Ramanan, Appl. Phys. Lett. 74 (1999) 1305.
[16] K. Narita, J. Yamasaki, H. Fukunaga, IEEE Trans. Magn. 16 (1980) 435.
[17] A. Zhukov, V. Zhukova, J.M. Blanco, A.F. Cobeño, M. Vazquez, J. Gonzalez, J. Magn. Magn. Mater. 258–259 (2003) 151.